Applied Soft Computing 69 (2018) 426–434

Contents lists available at ScienceDirect

Applied Soft Computing

journal homepage: www.elsevier.com/locate/asoc

A hybrid dermoscopy images segmentation approach based on neutrosophic clustering and histogram estimation

Amira S. Ashour[a], Yanhui Guo[b], Enver Kucukkulahli[c], Pakize Erdogmus[d], Kemal Polat[e,*]

[a] Department of Electronics and Electrical Communications Engineering, Faculty of Engineering, Tanta University, Tanta, Egypt
[b] Department of Computer Science, University of Illinois at Springfield, Springfield, Illinois 62703, USA,
[c] Department of Computer Technologies, Duzce Vocational School, Duzce University, 81620, Duzce, Turkey,
[d] Department of Computer Engineering, Faculty of Engineering, Duzce University, Duzce, Turkey,
[e] Department of Electrical and Electronics Engineering, Faculty of Engineering and Architecture, Abant Izzet Baysal University, 14280 Bolu, Turkey

ARTICLE INFO

Article history:
Received 26 January 2018
Received in revised form 2 April 2018
Accepted 2 May 2018
Available online 5 May 2018

Keywords:
Dermoscopy images
Skin lesion
Neutrosophic clustering
Image histogram
Image segmentation
Neutrosophic c-means clustering
Histogram based cluster estimation (HBCE)

ABSTRACT

In this work, a novel skin lesion detection approach, called HBCENCM, is proposed using histogram-based clustering estimation (HBCE) algorithm to determine the required number of clusters in the neutrosophic c-means clustering (NCM) method. Initially, the dermoscopic images are mapped into the neutrosophic domain over three memberships, namely true, indeterminate, and false subsets. Then, an NCM algorithm is employed to group the pixels in the dermoscopy images, where the number of clusters in the dermoscopy images is determined using the HBCE algorithm. Lastly, the skin lesion is detected based on its intensity and morphological features. The public dataset (ISIC 2016) of 900 images for training and 379 images for testing are used in the present work. A comparative study of the original NCM clustering method is conducted on the same dataset. The results showed the superiority of the proposed approach to detect the lesion with 96.3% average accuracy compared to the average accuracy of 94.6% using the original NCM without HBCE algorithm.

1. Introduction

Malignant melanoma is recorded a fatal skin cancer type worldwide. Earlier diagnosis can reduce the metastatic risk [1]. The dermoscopy technology improves the accuracy of skin lesion detection and the diagnostic of melanoma. Automated image analysis techniques of the dermatoscopic images become a critical issue in skin lesion detection. These techniques consist mainly of several stages, namely image acquisition, lesion border detection/segmentation, feature extraction, and classification. During these stages, the dermoscopic images segmentation and detection methods have a significant role that affects the effectiveness of the subsequent stages for early skin cancer identification.

Several dermoscopic segmentation algorithms have been established. Grana et al. [2] applied an automatic thresholding technique using Otsu's threshold to segment the melanoma images. The zero-crossings approach of a Laplacian of Gaussian (LoG) edge has been proposed by Rubegni et al. [3] to segment dermoscopy images. The smooth transition between the lesion and the nearby skin degraded the performance of the contour and edge-based methods due to such indistinct lesion boundaries. Thus, Zhou et al. [4] detected the lesion boundaries using a modified snake model based on region-based approaches. Gao et al. [5] proposed multi-resolution Markov random fields on dermoscopic images segmentation, while Zhou et al. [6] applied an anisotropic mean shift based fuzzy c-means approach. Nevertheless, in the presence of different colors or textured skin/lesion regions, region-based methods become complex and over-segmentation may occur. Consequently, several color clustering algorithms have been evaluated by Melli et al. [7], namely k-means, median cut, fuzzy c-means and mean shift, where the mean shift approach proved its superiority in term of specificity and sensitivity. This is due to the ability of the mean shift to adapt itself to the target image's features, which allowed it to produce clusters with more distant to each other in the feature space. The results established that the best obtained detected boundaries were with 64 for mean shift, and 6 clusters for k-means, fuzzy c-means, and the median cut.

Recently, several segmentation techniques based on the fuzzy set theory have been conducted to handle the uncertainty. The fuzzy c-means (FCM) can be applied to segment the images into sev-

* Corresponding author.
E-mail addresses: amirasashour@yahoo.com (A.S. Ashour), guoyanhui@gmail.com (Y. Guo), enverkulahli@gmail.com (E. Kucukkulahli), pakizeerdogmus@duzce.edu.tr (P. Erdogmus), kpolat@ibu.edu.tr (K. Polat).

https://doi.org/10.1016/j.asoc.2018.05.003
1568-4946/

eral regions using the pixels' membership values, which is robust to the skin tone variations and the shadow effect. Lee and Chen [8] implemented a skin cancer segmentation method using the FCM clustering, which provided superior results compared to Otsu's algorithm. Moreover, in order to handle the indeterminacy during the image processing, neutrosophy techniques, namely the neutrosophic set (NS) has been applied. A neutrosophic c-means (NCM) clustering method has been applied to cluster typical data points al data points for efficient data clustering and image segmentation. To reduce the set indeterminacy, Guo and Sengur [9] defined a directional operation (α-mean) in the neutrosophic color image, and then applied the modified FCM clustering method to the neutrosophic color image for segmentation. Guo and Sengur [10] incorporated the NS and FCM contexts to resolve the FCM incapability to handle uncertain data. Guo et al. [11] proposed efficient microscopic images segmentation using the NS and shearlet transform.

Typically, the clustering is an unsupervised learning procedure that requires either direct or indirect parameter's setting to specify the number of clusters/segments. These parameters need prior knowledge about the data in the image such as the number of clusters. In image segmentation, to determine the realistic number of clusters, several common approaches to estimate any model dimensions can be employed [12]. These approaches include the permutation tests, cross-validation, resampling, penalized likelihood estimation, and defining the error curve's knee. In practice, to determine the optimal number of clusters several studies have been conducted. Pei et al. [13] proposed an optimal method based on the inter-class and intra-class difference to select the number of clusters. Küçükkülahlı et al. [14] performed the segmentation process and selected the optimal number of clusters by examining the histogram both horizontally and vertically to record the local and global maximum values. The obtained probable clusters' centroids and the optimal number of clusters from the histogram have been used for further segmentation using k-means clustering.

In addition, lesion detection on Android platform has been implemented by Mendi et al. [15] in dermoscopy images. On the binary image, a density based clustering (DBSCAN) has been used to group the black pixels generated to discover cluster of arbitrary shapes. The authors used only the histogram equalization to increase the global contrast. Then, the FCM have been applied to segment the lesions. This study was focused only on the implementation of the Windows Phone and Android platforms. Another study has been conducted by Doğanay et al. [16] to extract the lung boundaries by combining the FCM and morphological operations. The FCM used the image's histogram for updating the fuzzy membership functions instead of using the image pixels. The image histogram was divided into the clusters rather than dividing the original image according to intensity values, and then the fuzzy membership function were calculated. However, the authors did not use the histogram information to determine the number of clusters and their centroids and handled only the image of the histogram.

Jalal Deen et al. [17] implemented a colored histogram-based FCM method (HTFCM), where an initialization of the cluster centroids has been initialized and determined using the histogram information in the color. For each histogram red, green and blue components, the cluster centroids have been initialized not the pixels. Then, a pre-segmentation process has been applied using the WaterShed algorithm. A histogram reconstruction by merging the three-components of the histograms, and multi-thresholding has been performed. This process was again used to produce a new histogram using some dominant valleys obtained from the used peak-valley location method in each component histogram, from which an initial cluster centroids were attained by the HTFCM procedure. However, these initial cluster centroids are influenced by three control parameters and an irrationality degree. Consequently, the clustering performance of the Jalal Deen et al. method is still restricted by the parameter selection problem and the complexity of using the three histogram components when using the colored histogram components.

Simultaneously, the dermoscopic images have some characteristics that complicated the segmentation process, namely [18], the fuzzy and irregular shape of the lesion's border, the low contrast in the transition between the lesion and its surrounding skin, the existence of several artifacts, such as the air bubbles, presence of hair, dissimilar lesion textures, shapes, sizes, and types, and variegated skin color in the lesion interior. These skin lesion characteristics produce several visual groups in the dermoscopic images. Thus, in the present work, the NCM is applied, where; it is considered an effective method at which each image's pixel fits in a cluster. Nevertheless, the proper determination of the number of clusters is often ambiguous as it depends on the scale and shape of the points' distribution in the image. Furthermore, increasing the number of clusters will continuously reduce the error in the subsequent clustering. Subsequently, the optimal determination of the number of clusters in the dermoscopic images will provide accurate clustering. Therefore, the determination of the correct value of the number of clusters is considered an essential process. In the current work, the procedure used in [14] is improved to fit the dermoscopic images' characteristics to determine the suitable number of clusters and the centers of these clusters based on the histogram. The proposed method uses the histogram information to efficiently improve the clustering performance. Afterwards, the NCM clustering is employed for further segmentation process. Thus, the proposed approach is called HBCENCM.

The remaining the current work is planned as follows. Section 2 includes the methodology of the proposed scheme, and then in Section 3. The results are discussed. Finally, in Section 4, the conclusion is drawn.

2. Methodology

Clustering is one of the most prevalent data analyses techniques, where the fuzzy c-means (FCM) clustering procedure is a well-known scheme in the segmentation process. The FCM allows any data point to fit two or more clusters instead of completely fitting to just one cluster as in the traditional k-means. Consequently, determining the number of clusters in the image has a significant role in the clustering process. Melanomas are serious skin lesions and identification by the naked eye requires the early-stage detection to distinguish them from benign type. Aiming to solve the problems in the skin lesion manual detection, this present work proposed a skin lesion automatic segmentation algorithm based on a predetermination of the number of clusters phase. Afterwards, the neutrosophic c-means (NCM) clustering algorithm is employed for the segmentation of the dermoscopy images.

2.1. Histogram-based number of clusters determination

The histogram is considered one of the reasonable tools to define the frequency distribution of the data in an image that represents the number of pixels at each different intensity value in the image. The X-axis in the histogram represents the bins, which are the set of the non-overlapping intervals representing the pixels' intensities in an image, while the Y-axis represents the count of the bins (number of pixels that have the corresponding intensity value). Hypothetically, the histogram will specify a peak for each cluster in the image. Thus, among the local maximum points, the centers of the clusters can be identified by comparing the horizontal and vertical distances [19].

Since image segmentation is based on separating the image into dissimilar regions, the grayscale histogram-based approach is broadly applied to this task due to its low computational complexity. Nevertheless, the traditional grayscale histogram-based approaches may lead to inaccurate segmentation due to the absence of the spatial information and the sharp details/irregularities on the grayscale histogram. Consequently, the present work determined the number of clusters based on interpreting the histogram of the dermoscopic image, where the candidate clusters' centroids are determined also by searching the histogram both horizontally and vertically. In the current work, all peaks and valleys in the image's histogram are identified to interpret the histogram information. Then, the distance between each peak points on the histogram and the succeeding valley is calculated to determine the clustering. A point is recorded as peak point if a decrease occurs from an increase in the recorded values; else, the point is considered a valley point if there is an increase from decrease. The values above the average are allocated as cluster starting values, and their number represents the number of clusters. In this study, the histogram-based clustering estimation is called HBCE algorithm, which calculates the number of clusters in an image as well as the estimated cluster centers.

In the proposed method, the dermoscopic image is converted to grayscale that has a histogram of 256 intensity values. Subsequently, the HBCE algorithm is applied using either the horizontal-vertical (h-v) procedure or the vertical- horizontal (v-h) procedure to determine the required clusters' number and their centroids. The horizontal-vertical procedure denotes the peaks and valleys based on the intensity values' transition from the high to low, while, the vertical-horizontal one considers the peaks' and valleys' transition based on the change in the number of pixels (counts) at each gray scale level. The HBCE pseudo-code to determine the cluster counts and their corresponding centers are as follows.

Algorithm: Histogram-based clustering estimation (HBCE)

Start
- ***Convert*** the dermoscopic images into gray scale
- ***Represent*** the images using its histogram
- ***Determination*** of peak and pit points in histogram either horizontal-vertical or vertical-horizontal
- ***Scan*** the histogram at vertical
- ***Exclude*** the smaller values compared to the average value
- ***Compute*** the average of distances between each peak and the subsequent pit
  - ***If*** the absolute difference between each point with succeeding one at peak and valley points is above the average
    - ***Record*** only the peak point at the maximum peaks
  - ***Endif***
- ***Scan*** the histogram horizontally
- ***Exclude*** the values smaller than average value
- ***Determine*** the places of the histogram of the maximum peaks by calculating the following value within the whole histogram
- *Total*=absolute distance of each maximum peak point with the next one multiplied by the value
- *Average*= Total/length of the places vector
  - ***If*** Total> Mean
    - ***Record*** the great value to the result
  - ***Endif***
- ***Determine*** the number of clusters
- ***Determine*** the clusters centers

Stop

2.2. Neutrosophic c-means clustering

Generally, the neutrosophy is employed to describe the uncertainty/indeterminacy information. In the present work, the neutrosophic set (NS) is combined with the clustering process to interpret the indeterminacy on the image for image segmentation [20]. In the NS theory, three sets representing the degrees of the truth (T), indeterminacy (I), and falsity (F) are included. In the NS domain, each pixel $A(i,j)$ in an image is signified as:

$$A_{NS}(i,j) = \{T(i,j), I(i,j), F(i,j)\} \tag{1}$$

where the membership functions $T(i,j)$, $I(i,j)$ and $F(i,j)$ represent the foreground, indeterminate set, and background, respectively. These membership sets can be computed as functions of the pixel intensity value $nn(x,y)$ and the gradient magnitude value $G_r(x,y)$ at the pixel(x,y) on the image as follows:

$$T(x,y) = \frac{nn(x,y) - nn_{\min}}{nn_{\max} - nn_{\min}} \tag{2}$$

$$I(x,y) = \frac{G_r(x,y) - G_{r_{\min}}}{G_{r_{\max}} - G_{r_{\min}}} \tag{3}$$

$$F(x,y) = \frac{nn_{\max} - nn(x,y)}{nn_{\max} - nn_{\min}} \tag{4}$$

where $G_r(x,y)$ and $nn(x,y)$ are the gradient and intensity values; respectively at the pixel (x,y). The NCM clustering is applied for clustering the uncertain data, which is motivated by the FCM and the NS framework. For clustering with indeterminacy, the objective function is defined as follows [21]:

$$M(T,I,F,C) = \sum_{i=1}^{N}\sum_{j=1}^{C}(\varpi_1 T_{ij})^m ||x_i - c_j||^2 + \sum_{i=1}^{N}(\varpi_2 I_i)^m ||x_i - \bar{c}_{i\max}||^2 + \sum_{i=1}^{N}\delta^2(\varpi_3 F_i)^m \tag{5}$$

where $\bar{c}_{i\max} = \frac{c_{pi}+c_{qi}}{2}$, $p_i = \underset{j=1,2,\cdots C}{arg\max}(T_{ij})$, and $q_i = \underset{j\neq p_i \cap j=1,2,\cdots C}{arg\max}(T_{ij})$ as p_i and q_i are the cluster numbers, and m is a constant. Once the p_i and q_i are known, the $\bar{c}_{i\max}$ is considered, which has a constant value for each data point i. T_{ij}, I_i and F_i are the membership values related to the defined clusters, indeterminate regions and the noisy data set, respectively, where $0 < T_{ij}, I_i, F_i < 1$, which satisfy with

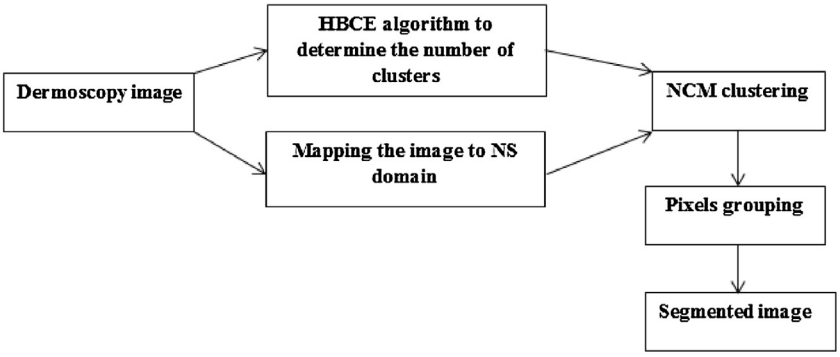

Fig. 1. Proposed HBCENCM block diagram.

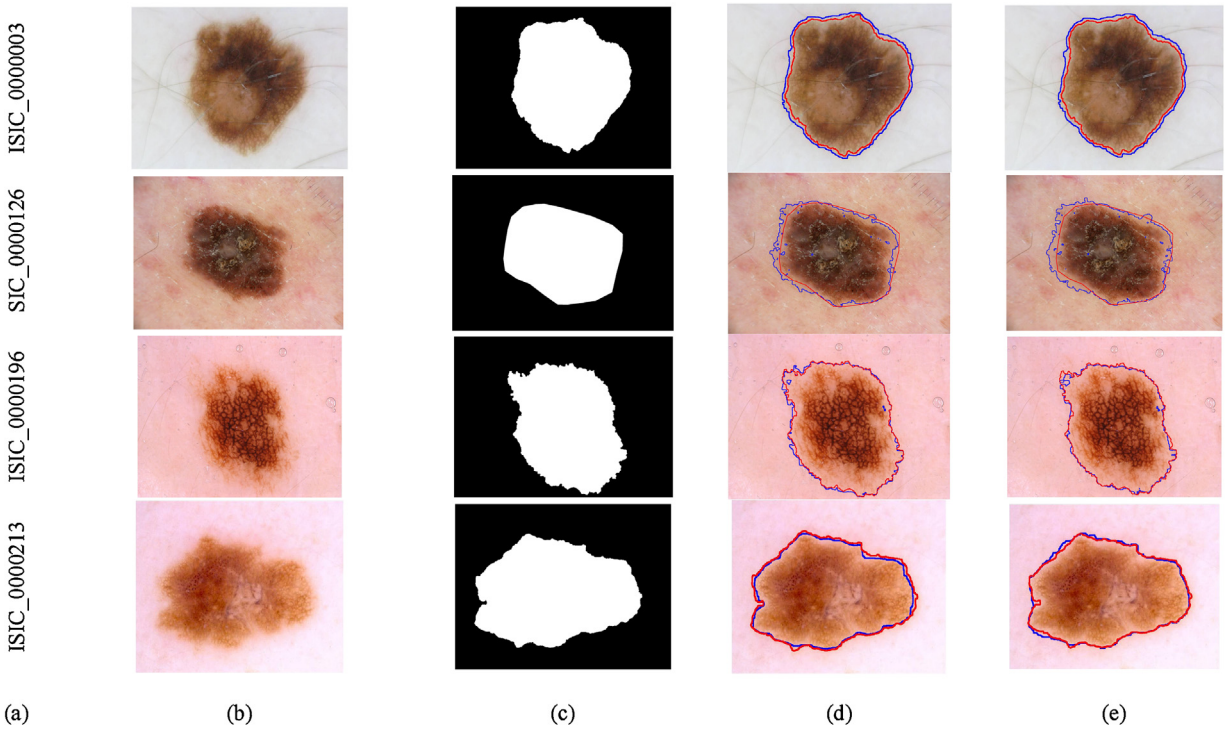

Fig. 2. Detection results of HBCENCM: (a) Dermoscopic image number, (b) Original skin lesion image, (c) Ground truth image, (d) Detected lesion region using the HBCE (h-v), (e) Detected lesion region using the HBCE (v-h).

$\sum_{j=1}^{C} T_{ij} + I_i + F_i = 1$. To minimize the objective function, T_{ij}, I_i and F_i can be updated as:

$$T_{ij} = \frac{K}{\varpi_1}\left(x_i - c_j\right)^{-\frac{2}{m-1}} \tag{6}$$

$$I_i = \frac{K}{\varpi_2}(x_i - \bar{c}_{i\max})^{-\frac{2}{m-1}} \tag{7}$$

$$F_i = \frac{K}{\varpi_3}\delta^{-\frac{2}{m-1}} \tag{8}$$

$$K = \left(\frac{\lambda_i}{m}\right)^{\frac{1}{m-1}} \tag{9}$$

In the current work, the neutrosophic image after determining the number of clusters is used as the input to the NCM clustering algorithm for skin lesion segmentation. Firstly, the colored skin lesion images are converted to grayscale image to apply the HBCE algorithm. Using the determined number of clusters and the NCM, the pixels in the dermoscopic images are clustered into several groups based on their true membership values as illustrated in Fig. 1.

Based on the characteristics of the lesions' intensity, the cluster with the lowest value of center is considered lesion candidate pixels. A connected component analysis is performed to extract the morphology features of the components. The final lesion is identified as the region with the biggest area.

3. Experimental results and discussion

In the present work, the International Skin Imaging Collaboration (ISIC) Archive [22] encloses skin lesions dermoscopic images, which consists of nine-hundred training images in the training set and 379 images in the test set. In the current work, 900 images are used for training to tune the proposed HBCENCM algorithm, and the 379 images are used for testing and to calculate the performance evaluation metrics (their mean and standard deviation) values. The available ground truth images are used to evaluate the detection results during the training and testing phases. The skin lesion detection results using the proposed HBCENCM approach

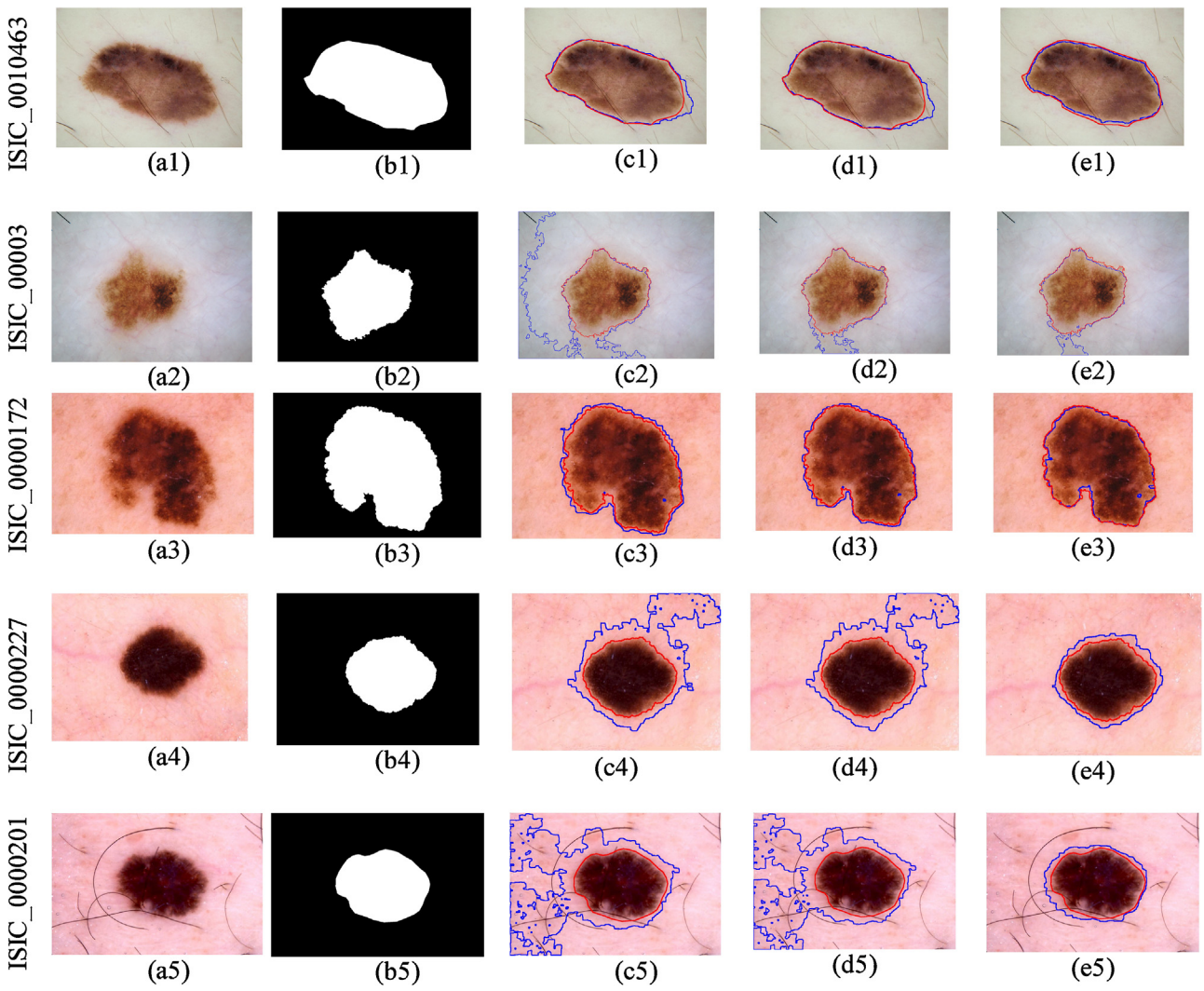

Fig. 3. Comparative segmentation results, where (a1–a5): original dermoscopic test images, (b1–b5): ground truth images, (c1–c5): segmented images using NCM algorithm, (d1–d5): HBCENCM proposed approach using v-h, and (e1–e5): HBCENCM proposed approach using h-v procedure.

in comparison with the ground truth images are demonstrated in Fig. 2. In Fig. 2c and d, the HBCE in the proposed method is used using the h-v and the v-h procedures; respectively. The detected boundaries are marked in blue, while the ground truth results are in red. The detected boundaries are nearly matched with the ground truth results.

Fig. 2 illustrates the accurate skin lesion regions detection using the HBCENCM approach even with different lesion shapes and sizes. Using h-v procedure achieves superior detection compared with the v-h procedure. The proposed HBCENCM is compared with the NCM clustering algorithm without pre-determination of the number of clusters for different image samples with different light illumination, size, shape, skin surface roughness/smoothness, and the existence of air bubbles. Fig. 3(a1–a5), (b1–b5), (c1–c5), (d1–d5), and (e1–e5) illustrate the original dermoscopic images, ground truth images, segmented images using the NCM algorithm only without HBCE, and the proposed HBCENCM approach using the h-v procedure, and the proposed approach using the v-h procedure, respectively.

Fig. 3 illustrates the superiority of the HBCENCM using the h-v procedure compared to the NCM without pre-determination of the number of clusters for detecting the skin lesion accurately. In order to evaluate the proposed HBCENCM approach, several performance metrics are measured. These metrics are the accuracy,

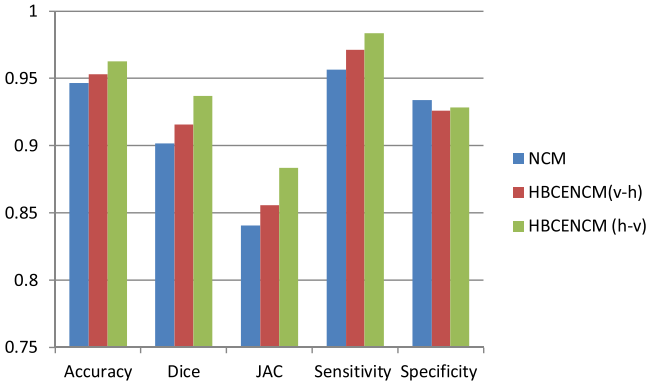

Fig. 4. Comparative evaluation metrics of five images using the NCM, HBCENCM (v-h), and HBCENCM (h-v).

Jaccard index (JAC), Dice coefficient, sensitivity, and specificity [23]. Consider TP refer to the true positives, TN refers to the true negatives, FP refers to the false positives, and FN refers to the false negatives. Then, in order to accurate evaluation to the proposed method using the h-v procedure and the v-h procedure against the original NCM algorithm, several evaluation metrics are measured, which are as follows: i) The Jaccard similarity index (JAC), which

Table 1
The average ± SD of the performance metrics of the proposed HBCENCM method with reference to ground truth boundaries.

Segmentation Method		Accuracy (%)	Dice (%)	JAC (%)	Sensitivity (%)	Specificity (%)
NCM		94.6329 ± 5.8	90.1626 ± 14.1	84.0564 ± 15.8	95.65 ± 6.4	93.3808 ± 13.2
Proposed Method	v-h procedure	95.3182 ± 4.2	91.5693 ± 10.3	85.556 ± 12.07	97.1269 ± 4.37	92.6153 ± 10.8
	h-v procedure	**96.281 ± 2.7**	**93.696 ± 3.4**	**88.336 ± 6.1**	**98.354 ± 2.2**	**92.845 ± 6.9**

The bold values are the highest values in the table.

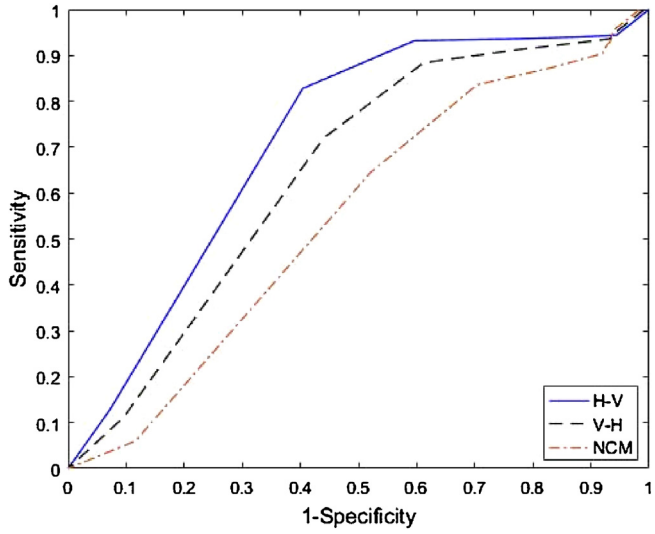

Fig. 5. Segmentation evaluation using the ROC curve.

is the most distinctive ratio between the intersection and union of the segmented image and the ground truth, ii) the Dice similarity index, which is slightly different than the JAC, but more commonly used, ii) Sensitivity = TP/(TP + FN), which measures the overlaps, iv) Specificity = TN/(TN + FP), which is the complement of the sensitivity, and the v) receiver operating characteristic (ROC) curve, which is based on the TP that represents the intersection between the segmented image and the corresponding ground truth (GT) image, the FP representing the intersection between the segmented parts not overlapping the GT, the FN representing the missed parts of the GT, and the TN representing the image part beyond the union of the segmented image and the GT.

The performance of the proposed approach is compared to the NCM without applying the HBCE algorithm. Along with these metrics, the cumulative percentage (CP) plot that reports the measured metrics is included to compare the performance of the HBCENCM and the NCM algorithms. The average values of the accuracy, Jaccard index, Dice index, sensitivity, and specificity are measured for the segmented images in the test dataset. Table 1 reports evaluation metrics' average values and standard deviation (SD) of the automated HBCENCM results compared to the NCM.

Table 1 reveals that the proposed approach detected the skin lesion regions with about 96.3%, and 95.3% accuracies compared to the ground truth images using any of the h-v, and the v-h procedures; respectively in the HBCE. These results are superior to the use of the NCM without a prior determination to the number of clusters. In addition, the average values of the measured metrics show a slight superiority of using the h-v procedure over the v-h one. The comparative results of the evaluation metrics are plotted in Fig. 4 for the NCM without HBCE, the proposed HBCENCM using h-v, and the proposed approach using v-h; respectively.

Fig. 4 establishes the preeminence of the proposed approach compared to the NCM without HBCE method owing to the accurate determination of the exact number of clusters in each image, which is based upon the image structure and histogram. In addition,

Table 2
Comparative results of the running time.

	Average Handling Time for all images
HBCE using h-v procedure	0.912558 (msec)
Corresponding clustering using NCM	118.1114 (Sec)
HBCE using v-h procedure	0.88106434 (msec)
Corresponding clustering using NCM	268.6246263 (Sec)

The bold values are the highest values in the table.

using the h-v procedure in the HBCE algorithm is superior to the v-h procedure. Fig. 4 reports that the proposed method using the h-v procedure achieved the best performance metric values compared to the NCM without HBCE and the proposed method using the v-h procedure. Additionally, Fig. 5 illustrates the ROC curve of the three compared approaches showing the superiority of the proposed HBCENCM-h-v compared to the other approaches.

Furthermore, the evaluation metrics' cumulative percentages are measured using the NCM, the HBCE-NCM with (v-h), and the HBCENCM with (h-v); respectively as illustrated in Figs. 6 through 8. The percentage of the number of images that have the specified metric value and their corresponding metrical values are represented on the Y-axis and X-axis, respectively. Fig. 6 illustrates the cumulative percentage of the different metrics, namely the accuracy, dice value, JAC, sensitivity, and specificity, respectively of the NCM method.

Only 10% of the images using the NCM method have about 96% maximum performance with all metrics as illustrated in Fig. 6. Compared to the HBCENCM method using the v-h procedure, the cumulative percentages of the different metrics are illustrated in Fig. 7.

Fig. 7 reports that about 10% of the images achieved about 98% maximum performance with all metrics. However, about 95% cumulative percentages of the images have about 55% value with all metrics. Fig. 8 illustrates the cumulative percentage of the different metrics, namely the accuracy, Dice value, JAC, Sensitivity, and Specificity; respectively of the HBCENCM method using the h-v procedure.

Fig. 8 reports that about 12% of the images achieved about 99% maximum performance with all metrics. However, about 95% cumulative percentages of the images have about 80% value with all metrics. However, there are some failed when using the proposed HBCENCM approach. Such cases are characterized by dark black border of the image, dark small lesion within brighter region, or very small bright lesion as illustrated in Fig. 9.

In the present study, the preceding results and the implement of the proposed approach has been conducted using the following frame work specifications, MATLAB version R2016b on a machine with 4-core Intel(R) Core i5-5200U 2.7-GHz CPU, NVIDIA GEFORCE 920 M and 8 Giga RAM. The computational running time of the HBCENCM on the ISIC2016 testing dataset and when using HBCE alone and NCM alone are reported in Table 2.

Table 2 depicts that the h-v procedure took longer time compared to using the v-h procedure; however, the corresponding NCM with the h-v procedure took less time as the number of clusters determined by using the h-v procedure is less than those determined by the v-h procedure. Generally, the HBCE procedure does

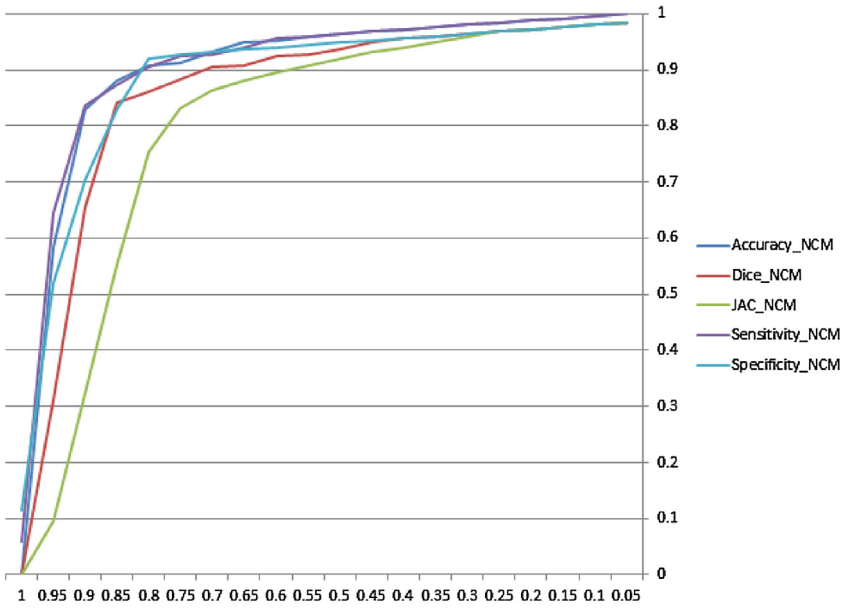

Fig. 6. The CP of the different metrics with using the NCM method.

Table 3
The corresponding computational time to the image size.

Image size (number of pixels per image)	HBCE (h-v) Average Handling Time (msec)	Corresponding NCM Average Handling Time(Sec)	HBCE (v-h) Average Handling Time (msec)	Corresponding NCM Average Handling Time(Sec)
441792	0.561767107	**30.9963732**	**0.36995372**	109.8566448
737038	1.770393872	**28.09717243**	**0.357594702**	43.65381313
786432	0.534667956	**41.95685255**	**0.393997423**	145.6798231
786432	0.97528063	**63.37979169**	**1.297262564**	107.5610092
786432	0.608348709	**143.7497587**	**0.492995651**	194.3894383
6096384	2.883156359	**260.5419264**	**8.599757795**	260.5419264
7077888	4.486506344	**489.7901111**	**0.866609923**	1643.640102
12212224	1.077886315	**691.1329361**	**1.461499091**	728.0653939

The bold values are the highest values in the table.

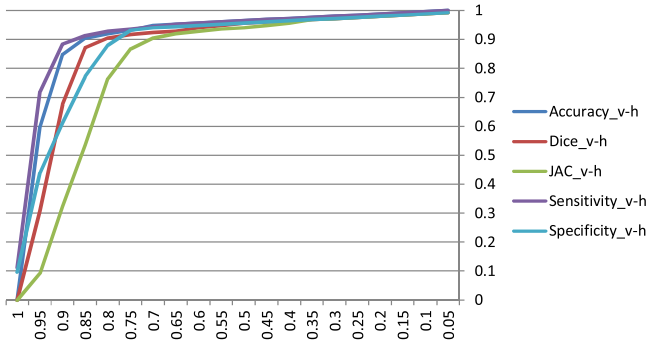

Fig. 7. The CP of the different metrics with using the HBCENCM method using with v-h procedure.

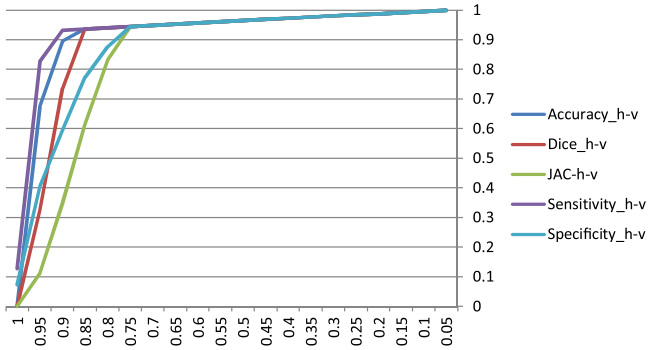

Fig. 8. The CP of the different metrics with using the HBCENCM method using with h-v procedure.

not take more than 10 msec to determine the required cluster number and their centroids. The HBCE algorithm does not depend on the number of pixel on the image and depends only on the distribution of the pixel on the image levels. However, the NCM takes much time, which are also increases linearly with the increasing in the number of pixels in an image (image size) as illustrated in Table 3.

Tables 2 and 3 illustrate that using the HBCE approach to determine the number of clusters either with the h-v procedure or the v-h procedure took very short time in msec. Finally, the proposed method is compared to the top recorded state-of-the-art lesion segmentation challenge's results that have been conducted on the ISIC2016 challenge. For melanoma recognition, Yu et al. [24] proposed a fully convolutional residual network (FCRN) integrating with a multi-scale contextual information structure on the ISIC2016 dataset. In addition, Bi et al. [25] introduces a parallel approach that combined the corresponding information resulting from individual segmentation phases for accurate localization of the lesion boundaries using theISIC2016 dataset. The simulation results reported 91.18% average Dice coefficient. Table 4 reported the metrics results comparison between the proposed HBCENCM using the h-v procedure and the top state-of-the-art methods in [24] and [25], which conducted on the same dataset.

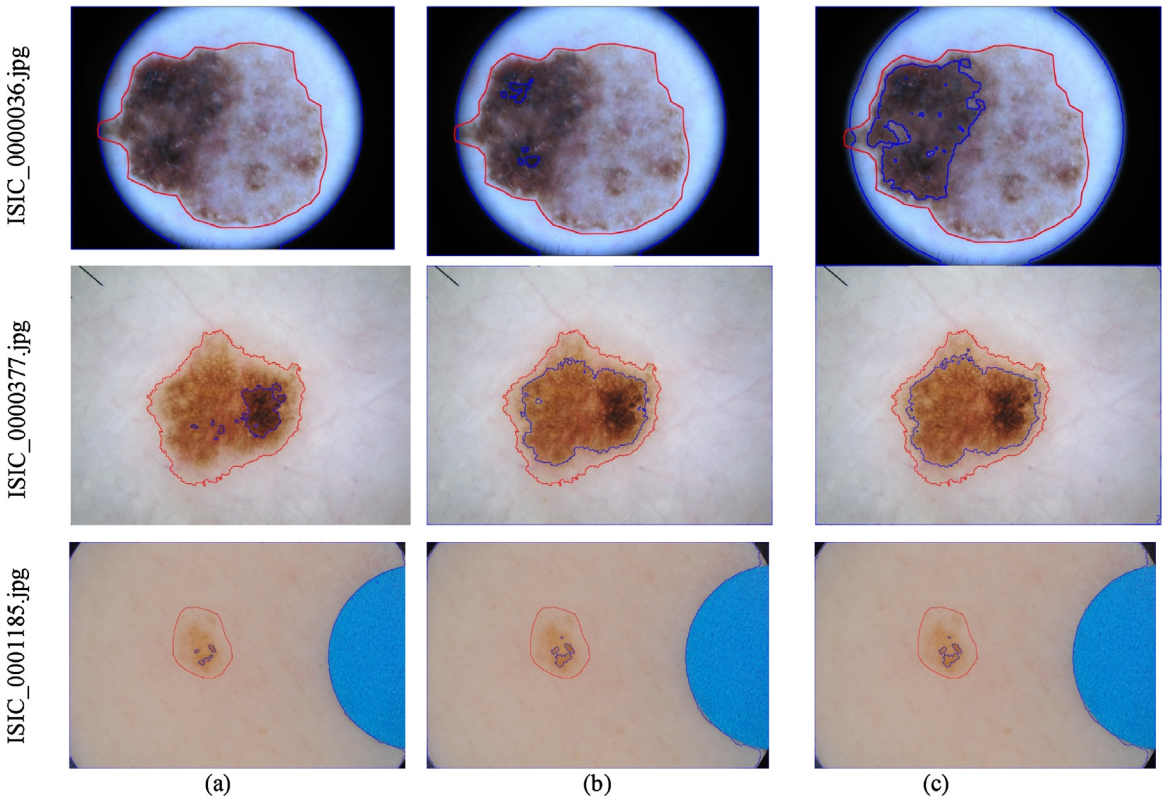

Fig. 9. Samples of failed segmentation cases using (a) the proposed HBCENCM with the h-v procedure, (b) using (a) the proposed HBCENCM with the v-h procedure, (c) using the original NCM method.

Table 4
Comparative study of the proposed HBCENCM using the h-v procedure and the state-of-the-art segmentation tasks on the ISIC 2016 dataset in terms of the performance metrics.

Method	Accuracy%	DICE%	JAC%	Sensitivity%	Specificity%
ISIC2016-Part1 (Yu et al. [19])	95.30	91.00	84.30	91.00	96.50
ISIC2016-Part1 (Bi et al. [20])	95.50	91.18	84.60	92.00	96.50
Proposed HBCENCM (h-v procedure)	96.281	93.696	88.336	98.354	92.845

Table 4 established the superiority of the proposed HBCENCM using the h-v procedure, where the compared with the deep learning based methods, the proposed method considered the characteristics of the dermoscopic images. In addition, it does not need many images for training.

The above results show the superiority of the proposed HBCENCM with the horizontal-vertical procedure with 96.3% accuracy over using the vertical-horizontal procedure as well as the NCM without HBCE. This result is due to the differences in the lesion region pixels intensity from type to another, where, using the horizontal-vertical procedure gives the impact to the pixels' intensity in the histogram. Consequently, it to increase the impact of the proposed method in terms of the algorithmic development in the field, it is recommended to apply the proposed method in the medical practice for decision support as a future work. In addition, it is recommended to study resolve the excluded failed cases.

4. Conclusion

The main core of this proposed method is the use of the dermoscopic images' histogram to determine the required number of clusters for further segmentation process. Thus, the skin lesion detection procedure is based on the HBCE procedure and the neutrosophic c-means (NCM). The number of clusters in the dermoscopy images is determined according to the histogram of each image, and based on the segmentation regions' intensities, the lesion is recognized. The ISIC 2017 data set is used for training and testing the proposed HBCENCM. Randomly selected two hundred images were used for training and seven hundred images for testing. The evaluation metrics established the superiority of the proposed HBCENCM with the horizontal-vertical procedure for detecting and segmenting the skin lesion compared with the NCM method. The proposed HBCENCM with h-v achieved average 96.3% accuracy even with images of different uniformity, size, shape, color, and light illumination as well as in the presence of the air bubbles.

References

[1] R. Siegel, E. Ward, O. Brawley, A. Jemal, Cancer statistics, 2011, CA. Cancer J. Clin. 61 (4) (2011) 212–236.
[2] C. Grana, G. Pellacani, R. Cucchiara, S. Seidenari, A new algorithm for border description of polarized light surface microscopic images of pigmented skin lesions, IEEE Trans. Med. Imaging 22 (8) (2003) 959–964.
[3] P. Rubegni, A. Ferrari, G. Cevenini, D. Piccolo, M. Burron, et al., Differentiation between pigmented spitz naevus and melanoma by digital dermoscopy and stepwise logistic discriminant analysis, Melanoma Res. 11 (1) (2001) 37–44.
[4] H. Zhou, G. Schaefer, M.E. Celebi, F. Lin, T. Liu, Gradient vector flow with mean shift for skin lesion segmentation, Comput. Med. Imaging Graph. 35 (2) (2011) 121–127.
[5] J. Gao, J. Zhang, M.G. Fleming, A novel multiresolution color image segmentation technique and its application to dermatoscopic image

segmentation, in: Proceedings of the IEEE International Conference on Image Processing, Vancouver, BC, Canada, September, 2000.
[6] H. Zhou, G. Schaefer, A.H. Sadka, M.E. Celebi, Anisotropic mean shift based fuzzy c-means segmentation of dermoscopy images, IEEE J. Sel. Top. Signal Process. 3 (1) (2009) 26–34.
[7] R. Melli, C. Grana, R. Cucchiara, Comparison of color clustering algorithms for segmentation of dermatological images, San Diego, in: Proceedings of the SPIE Conference on Medical Imaging, vol. 3S1-9, 2006.
[8] H. Lee, Y.P.P. Chen, Skin cancer extraction with optimum fuzzy thresholding technique, Appl. Intell. 40 (3) (2014) 415–426.
[9] Y. Guo, A. Sengur, A novel color image segmentation approach based on neutrosophic set and modified fuzzy c-means, Circ. Syst. Signal Process 32 (4) (2013) 1699–1723.
[10] Y. Guo, A. Sengur, NCM: Neutrosophic c-means clustering algorithm, Pattern Recogn. 48 (8) (2015) 2710–2724.
[11] Y. Guo, A.S. Ashour, B. Sun, A novel glomerular basement membrane segmentation using neutrsophic set and shearlet transform on microscopic images, Health Inf. Sci. Syst. 5 (1) (2017) 15.
[12] S. Salvador, P. Chan, Determining the number of clusters/segments in hierarchical clustering/segmentation algorithms, in: 16th IEEE International Conference on Tools with Artificial Intelligence, 2004. ICTAI 2004, IEEE, November, 2004, pp. 576–584.
[13] J. Pei, L. Zhao, X. Dong, X. Dong, Effective algorithm for determining the number of clusters and its application in image segmentation, Cluster Comput. 20 (4) (2017) 2845–2854.
[14] E. Küçükkülahli, P. Erdoğmuş, K. Polat, Histogram-based automatic segmentation of images, Neural Comput. Appl. 27 (5) (2016) 1445–1450.
[15] Engin Mendi, Caner Yogurtcular, Yusuf Sezgin, Coskun Bayrak, Automatic mobile segmentation of dermoscopy images using density based and fuzzy c-means clustering, IEEE International Symposium on Medical Measurements and Applications (MeMeA) (2014).
[16] Emine Doğanay, Sadık Kara, Hatice Kutbay Özçelik, Levent Kart, A hybrid lung segmentation algorithm based on histogram-based fuzzy C-means clustering, Computer Methods in Biomechanics and Biomedical Engineering: Imaging & Visualization.
[17] K. Jalal Deen, R. Ganesan, A. Merline, Fuzzy-C-means clustering based segmentation and CNN-classification for accurate segmentation of lung nodules, Asian Pac. J. Cancer Prev. 18 (7) (2017) 1869–1874, http://dx.doi.org/10.22034/APJCP.2017.18.7.1869.
[18] M.E. Celebi, H. Kingravi, H. Iyatomi, A. Aslandogan, W.V. Stoecker, R.H. Moss, Border detection in dermoscopy images using statistical region merging, Skin Res. Technol. 14 (3) (2008) 347–353.
[19] D. Hao, Q. Li, C. Li, Histogram-based image segmentation using variational mode decomposition and correlation coefficients, Signal Image Video Process. 1–8 (2017).
[20] F. Smarandache, Neutrosophy. Neutrosophic Probability, Set, and Logic, ProQuest Information & Learning, Infolearnquest, Ann Arbor, MI, USA, 1998, p. 105.
[21] Y. Guo, R. Xia, A. Şengür, K. Polat, A novel image segmentation approach based on neutrosophic c-means clustering and indeterminacy filtering, Neural Comput. Appl. (2016) 1–11.
[22] International Skin Imaging Collaboration Website. http://www.isdis.net/index.php/isic-project.
[23] Y. Guo, C. Zhou, H.P. Chan, A. Chughtai, J. Wei, L.M. Hadjiiski, E.A. Kazerooni, Automated iterative neutrosophic lung segmentation for image analysis in thoracic computed tomography, Med. Phys. 40 (8) (2013).
[24] L. Yu, H. Chen, Q. Dou, J. Qin, P.A. Heng, Automated melanoma recognition in dermoscopy images via very deep residual networks, IEEE Trans. Med. Imaging 36 (4) (2017) 994–1004.
[25] L. Bi, J. Kim, E. Ahn, A. Kumar, M. Fulham, D. Feng, Dermoscopic image segmentation via multistage fully convolutional networks, IEEE Trans. Biomed. Eng. 64 (9) (2017) 2065–2074.